Textile Research Journal

Original article

Modeling to predict thermal aging for flame-retardant fabrics considering thermal stability under fire exposure

Textile Research Journal
2021, Vol. 91(21–22) 2656–2668

DOI: 10.1177/00405175211013835
journals.sagepub.com/home/trj
SAGE

Xiaohan Liu[1], Miao Tian[1,2], Yunyi Wang[1,2], Yun Su[1,2] and Jun Li[1,2]

Abstract

The performance of firefighters' clothing will deteriorate due to various exposures. Predicting its service life before decommissioning is essential to guide the use and maintenance of the uniform. The aim of this study is to introduce a model to predict the tensile strength of flame-retardant fabrics under fire exposure. The thermal degradation and microstructure of Kevlar/polybenzimidazole and polyimide/Kevlar fabrics were investigated. The decrease of tensile strength was attributed to the chemical changes and the development of microstructure cracks and charring of the fibers. Multiple linear regression (MLR) and artificial neural network (ANN) models were established to predict the tensile strength after thermal aging. The ANN model presented a better prediction result ($R^2 = 0.88$, root mean square error (RMSE) = 96.91) than the MLR method ($R^2 = 0.76$, RMSE = 138.61). The addition of fabric backside temperature (T), glass transition temperature (T_g), and degradation temperature (T_d) further increased the R^2 (4%) and decreased the RMSE (14.99) of the ANN model, which was recommended as a prediction approach with better accuracy. The findings of this study will contribute to estimating the continuous performance of firefighting clothing.

Keywords

Flame-retardant fabric, thermal aging, mechanical properties, thermal stability, artificial neural network

Thermal protective clothing is widely used in the manufacture of fire service uniforms and high-temperature working uniforms to protect firefighters or industrial workers from thermal hazards by providing insulation against heat transmission to human skin.[1–3] The firefighting suit is designed as a multi-layer structure, including an outer shell, moisture barrier, and a thermal liner, all of which are flame-retardant. Various standards clearly specify the minimum requirements for the performance of firefighting clothing; however, there are no clear guidelines for its continuous use. In order to understand how the performance of firefighting clothing changes over time, non-destructive techniques were used and prediction models were developed.[4]

For non-destructive testing, previous research has focused on the application of empirical equations. However, due to the complex mathematical relationships between them, these empirical equations may be limited in practical applications.[5] Therefore, the prediction model was developed by researchers to predict the performance of fabrics after thermal aging. Among them, the multiple linear regression (MLR) model was most widely used. Rezazadeh and Torvi[6] used regression analysis to establish a linear equation between the reflection coefficient and tensile strength of flame-retardant fabrics to predict the tensile strength of fabrics after thermal aging; some researchers have

[1]College of Fashion and Design, Donghua University, China
[2]Key Laboratory of Clothing Design and Technology, Donghua University, Ministry of Education, China

Corresponding authors:
Miao Tian, College of Fashion and Design, Donghua University, No. 1882, West Yan-An Road, Shanghai 200051, China.
Email: tianmiao@dhu.edu.cn

Jun Li, College of Fashion and Design, Donghua University, No. 1882, West Yan-An Road, Shanghai 200051, China.
Email: lijun@dhu.edu.cn

established a MLR model for predicting the tensile strength of the fabric under radiant thermal aging conditions.[7] Although the MLR model can predict the performance of the fabric, the artificial neural network (ANN) model shows higher prediction accuracy.[8] These models were commonly used for different exposures under thermal radiation conditions. However, the investigation of factors impacting the aging of flame-retardant fabrics has focused on heat, light, humidity, etc.[9–11] Firefighters who frequently perform rescue tasks also encounter flames in the firefighting operation. Due to the fundamental differences between flame and pure radiation heat transfer, the thermal aging mechanism of the fabrics may be different as well.[12] A convective heat flux of 80 kW/m^2 was applied to six types of firefighting clothing fabric systems, and the changes in the mechanical properties of the fabrics were analyzed,[13] but there was no predictive study on the mechanical properties of the fabric.

After undergoing thermal aging, the properties of the flame-retardant fabrics would experience varying degrees of decline. The outer shell is the outermost layer of the firefighters' clothing, which directly contacts abrasive and sharp surfaces; hence, its thermal protection and mechanical properties are particularly important. High mechanical strength of the fabrics means less maintenance and replacement cost.[14] The strength of the outer shell will change and probably drop below the requirements specified by the standard due to various exposures. The index of tensile strength has been extensively used to evaluate the mechanical performance of outer shell specimens after heat exposures. X-fiper fabrics were exposed to a radiant heat source with low heat flux, and the mechanical properties of the fabrics decreased after thermal exposure. However, the thermal protection performance of the fabrics did not change significantly.[15] Vogelpol[14] performed tests on firefighting clothing samples after use, and a remarkable reduction of mechanical properties was observed. Besides, the NFPA 1971 standard indicated that the tensile strength of the outer shell of firefighting clothing shall not be less than 623 N, which was a typical index to characterize the aging of the fabrics.

The thermal aging process of the fabrics was affected by environmental factors, such as heat flux intensity, heat exposure time, and fabric type.[16–18] Under the condition of higher intensity heat flux, the fabric would undergo oxidative degradation and be destroyed.[19,20] The characteristic temperature of the fabric during the thermal aging process, such as the surface temperature, glass transition temperature, and degradation temperature, could explain the aging mechanism of fabrics to a certain extent. Mostly, the decline of mechanical properties of the flame-retardant fabrics could not be detected visually and physical tests are necessary to confirm the loss of mechanical properties after heat exposure.[21,22] Although standard test methods could accurately assess the changes in mechanical properties of the flame-retardant fabrics, it is difficult to evaluate the in-use garments through fabric testing. Therefore, an appropriate quantitative method was still needed to evaluate the principle of degradation of flame-retardant fabric flame exposure[23] and predict the mechanical strength of fabrics without destruction.

The purpose of this research was to investigate the degradation of the outer shell of firefighters' protective clothing caused by flame exposure, and to reveal the aging mechanism of the fabrics from a microscopic level. A MLR and an ANN model were established to predict the tensile strength of the fabric after thermal aging. The findings of this study will help evaluate the service life of firefighters' protective clothing.

Experimental details

Materials

In order to accurately simulate firefighters performing tasks in the real state time, a three-layer fabric system was used to implement the thermal aging simulation experiment. To avoid the additional effects of thermal shrinkage on the variation tendency of the properties, two flame-retardant blend fabrics commonly used as the outer layer of firefighters' protective clothing and that do not easily shrink were selected in this study.[24] Fabric A was provided by IBENA Shanghai Technical Textiles Co. Ltd (China) and Fabric B was provided by Dongguan Sheng Mao Special Weaving Co. Ltd (China). The original tensile strength of the two specimens was tested according to the standard ISO 13934-1-2013. The basic specifications are list in Table 1.

Experimental design

To evaluate the degradation of the outer shell of the fire protection clothing caused by flame exposure, only the Meker burners of the thermal protective performance (TPP) tester were activated to simulate a real fire scene. The specimens were cut with a size of 150 mm × 150 mm and the heat exposure area was 100 mm × 100 mm according to ISO 17492-2019. The specimens were placed in the warp direction during the test and five repeated experiments were performed. A schematic diagram of the test apparatus and the size of specimens are shown in Figure 1.

Heat fluxes of 30, 40, 50, and 60 kW/m^2 were set by controlling the gas flow of the TPP tester. Three calibrations were performed and the heat flux was

Table 1. The basic properties of flame-retardant fabrics

Fabric code	Number	Content	Weight (g/m^2)	Thickness (mm)	Structure	Tensile strength (N)
Outer shell	A	60% Para-aramid/40% polybenzimidazoles	200	0.37	Plain	1610 ± 12
	B	85% Polyimide/15% para-aramid	200	0.42	2/1 Twill	1307 ± 16
Moisture barrier	C	100% meta-aramid, Polytetrafluoroethylene (PTFE) film	108.2	0.52	Water thorn felt with PTFE	/
Thermal liner	D	100% Meta-aramid	96.7	1.31	Needle punched nonwoven	/

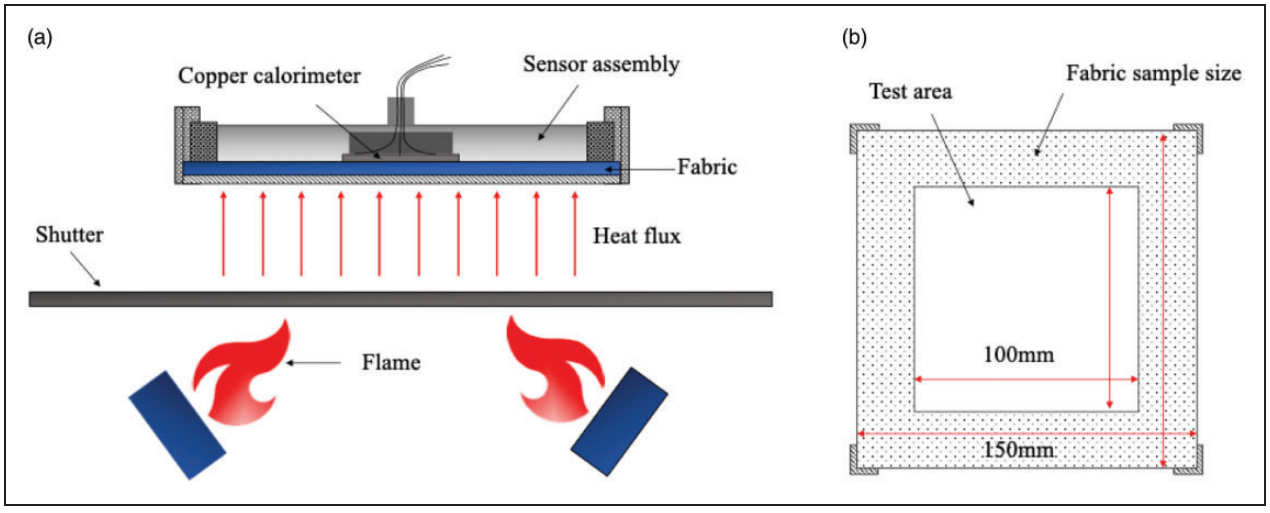

Figure 1. (a) Schematic diagram of the thermal protective performance tester. (b) Size of the specimens.

guaranteed by the copper calorimeter embedded in the TPP tester before thermal aging tests. This situation may cause a certain degree of damage, which might be difficult to detect through manual inspection, and it was impossible to decide whether to use firefighters' protective clothing further.[13] The heat flux density in this range had been used as the standard value for performance testing in different specifications.[23] As shown in Table 2, the flame duration was determined after the preliminary experiment, which was set as every 10 different times under different heat flux density to ensure the integrity of the fabric after flame exposure.

Table 2. Experimental design of thermal aging

Specimen	Heat flux (kW/m^2)	Exposure duration (s)
A + C + D	30	9, 11, 13, 15, 17, 19, 21, 23, 25, 27
	40	7, 9, 11, 13, 15, 17, 19, 21, 23, 25
	50	2, 4, 6, 8, 10, 12, 14, 16, 18, 20
	60	1, 2, 4, 6, 8, 9, 10, 12, 14, 15
B + C + D	30	7, 9, 11, 13, 15, 17, 19, 21, 23, 25
	40	4, 5, 6, 8, 10, 12, 14, 16, 18, 20
	50	1, 2, 4, 6, 8, 9, 10, 12, 14, 15
	60	1, 2, 3, 4, 5, 6, 7, 8, 9, 10

Methods

Testing methods

Measurement of fabric thermal stability. To obtain the thermal decomposition temperature of flame-retardant fabrics, and analyze the thermal stability of the fabrics, the relationship between thermal degradation and heat exposure was characterized using thermogravimetric analysis (TGA). TGA experiments in this research were conducted using a TG 209 F1 Libra. Specimens of approximately 7.5 mg were cut from each fabric and placed in a high-temperature ceramic crucible. The temperature was scanned from 30°C to 900°C at 10 K/min under nitrogen atmospheres. The data were

represented as a mass fraction and its derivative with time (DTG), as a function of temperature.

The glass transition temperature of fabrics was characterized using differential scanning calorimetry (DSC). DSC experiments in this research were conducted using a NETZSCH DSC 214. Specimens of approximately 5.5 mg were cut from each fabric and placed in a high-temperature aluminum crucible. The temperature was changed from 30°C to 500°C at 10 K/min under a nitrogen purge.

Scanning electron microscopy. A Dutch Phenom XL scanning electron microscope (SEM) was used to analyze the surface morphology of the fabrics, and to reveal the microstructure damage (such as pits, holes, cracks) of the fabric by comparing the unaged and aged shell specimens. The images were magnified by 200×, 1000×, and 3000× to observe the microstructure changes of the fabric.

Measurement of fabric surface temperature. A K-type thermocouple (Omega) with a diameter of 0.5 mm was used for temperature measurement during the thermal aging of specimens. The thermocouple was fixed on the back of the outer shell with flame-retardant wires, monitoring the temperature of the center point on the back of the outer shell. Specimens were exposed to the four heat fluxes for 60 s. The temperature of the fabric during heating and cooling phases was recorded by a Squirrel 2020 Grant data logger for120 s. The position of the thermocouple is shown in Figure 2.

Mechanical properties test. The tensile strength of exposed and unexposed samples was tested according to ASTM D5035. The Instron 3365 universal material testing machine (Instron Inc., USA) was used with a load capacity of 5 kN. The machine was a Constant-Rate-of-Extension (CRE) type, which operated at 300 mm/min. A fixed gauge length of 75 mm was used.

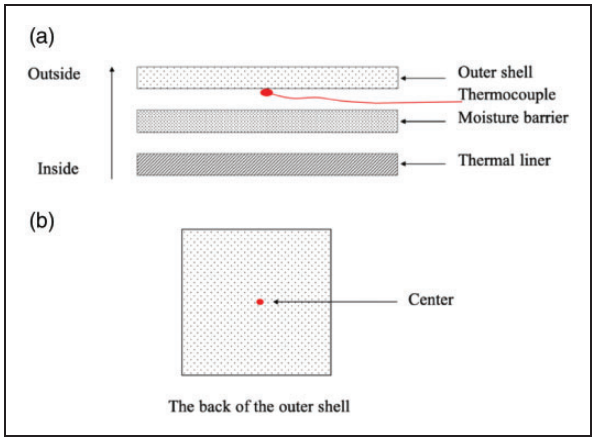

Figure 2. Schematic diagram of the thermocouple location.

Five samples in the warp direction were tested, and the average value and standard error were calculated.

Modeling methods

The different fabric performance indicators obtained through experiments were used as input parameters to predict the tensile strength of the fabric after thermal aging. In this study, MLR and ANN modeling methods were used. It was worth noting that too many or interdependent input variables (such as fabric characteristics) may interfere with the model, leading to variability in the predicted output.[25] The relationship between macro indicators (such as fabric type, heat exposure time, heat flux density, etc.) and the tensile strength after thermal aging was generally established in previous studies. However, the surface temperature profile, glass transition temperature, and degradation temperature were also characteristic parameters of the fabric, which could not be neglected. We explored the effect with considering the temperature rise indicators during thermal aging on the predictive performance of the model. Through correlation analysis, the key fabric characteristics used to predict tensile strength were determined and used as input variables in MLR modeling. A total of 400 experimental data were obtained in this study. Some 70% of the data were randomly allocated for training, 15% was used for verification, and the remaining 15% was used to test the performance of the model.

MLR modeling. The characteristic parameters of the fabric to predict the tensile strength of the fabric after thermal aging was used for MLR modeling. Equation (1) shows the general form of the MLR model

$$Performance = C + \beta_1 x_1 + \beta_2 x_2 + \cdots + \beta_n x_n \quad (1)$$

where C is the constant normal error of the same distribution; $\beta_1 \ldots \beta_n$ is the regression coefficient of the relative strength of each fabric performance; $x_1 \ldots x_n$ is the performance index of the fabric.

ANN modeling. The ANN is a powerful data modeling tool that can capture and represent any type of relationship between input and output variables.[26] A three-layer perceptron architecture was adopted, namely an input layer, a hidden layer, and an output layer. As shown in Equations (2) and (3), the hyperbolic tangent function and identity function were selected as the activation functions of the hidden layer and output layer of the model, respectively. These specific functions can be applied to all types of data and provide better performance for the ANN model.[27] Interconnection between the neurons of adjacent layers is provided by weights.[28]

The input layer is the properties of the fabric, and the output layer is the tensile strength of the fabric after flame heat aging. Usually, the challenge of using neural networks is to determine the number of neurons in the hidden layer. Too many or too few will result in inaccurate output. In order to get the best number of neurons in the hidden layer, the ANN model was trained with a different number of neurons, and the best prediction ANN model with seven hidden neurons was found. Figure 3 shows a schematic diagram of all networks

$$f(x) = \frac{\sin hx}{\cos hx} = \frac{e^{x} - e^{-x}}{e^{x} + e^{-x}} \quad (2)$$

$$f(x) = x \quad (3)$$

where x is the weighted sum of neuron input and $f(x)$ is the converted output of the neuron.

Performance evaluation. The prediction performance parameters of the model were compared by the determination coefficient R^2 and the root mean square error (RMSE). The model with higher R^2 and lower RSME value was considered to be a high-performance prediction model.[29,30] Equations (4) and (5) represent the mathematical formulas of R^2 and RMSE, respectively

$$R^2 = 1 - \frac{\sum_{k=1}^{n} (y_k - x_k)}{\sum_{k=1}^{n} (y_k - \bar{y})} \quad (4)$$

$$RMSE = \sqrt{\frac{\sum_{k=1}^{n} (y_k - x_k)^2}{n}} \quad (5)$$

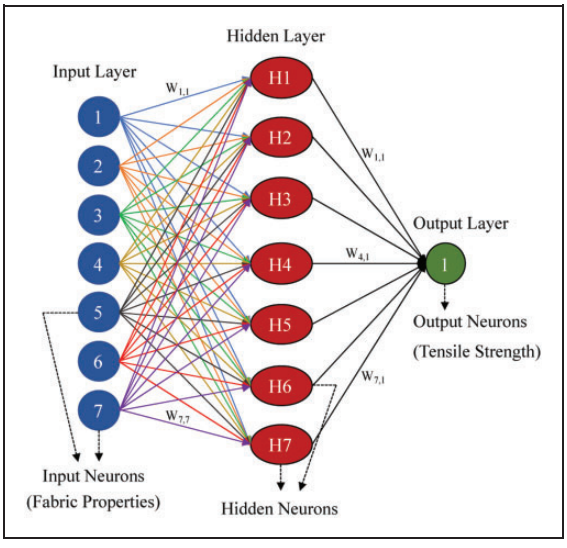

Figure 3. Schematic diagram of the artificial neural network model with seven input neurons, seven hidden neurons, and one output neuron.

where y_k is the experimental value, x_k is the predicted value, n is the total number of experimental values, and $\bar{y}$ is the mean of the experimental values.

Results and discussion

Thermal stability of the fabrics

TGA was performed on the selected samples. Figure 4 illustrates the thermogravimetry (TG) and differential thermal gravimetry (DTG) curves of fabrics A and B in a dry nitrogen atmosphere. During the initial period from 30°C to 100°C, both fabric A and fabric B have a slight mass loss (1–4%), due to the loss of bound water between fabric molecules. At 200–500°C, the dye started to fall off from the fabric gradually. As the temperature increases, the intermolecular forces gradually decrease, and the quality of fabric A decline slowly. When the temperature approaches 600°C, the fabric reaches the maximum thermal decomposition rate, and the mass loss elevates rapidly between 550°C and 650°C. The mass loss at this stage was about 35%, which was attributed to the pyrolysis of a large number of molecular chains into smaller molecules. Substances with a lower vaporization temperature were released,[23] and these mass losses correspond to the destruction of the fabric and the charring of the material. Fabric B reached the maximum thermal decomposition rate at 599.4°C. However, the TGA curve of fabric B was flat and began to drop sharply at the T_{onset} temperature. The surfaces of the fabric began to be carbonized and some fibers began to melt. Both fabric A and fabric B have higher thermal decomposition temperature, and the carbon residue was still close to 50% at 900°C.

Figure 5 reveals the DSC curve characteristics of fabrics A and B. The glass transition temperature was determined by the analysis software that came with the instrument (fabric A: 401.96°C; fabric B: 393.29°C). The amorphous polymer macromolecules in the fabric begin to forge freely. Its performance began to change sharply.[25] For the two fabrics, the difference in glass transition temperature showed little difference. Combined with the analysis in Figure 4, the glass transition temperature of the fabric appears at the beginning of degradation. After this stage, the quality loss of the fabric began to drop sharply.

In general, longer single exposure duration and higher heat flux caused lower tensile strength, which has been demonstrated in previous studies.[7,31] This was because the longer exposure and higher heat flux caused a higher temperature at the fabric surface and resulted in severer damage in the fabric. The results of TGA and DSC curves show that Kevlar/polybenzimidazole (PBI) and polyimide (PI)/Kevlar fabrics exhibit

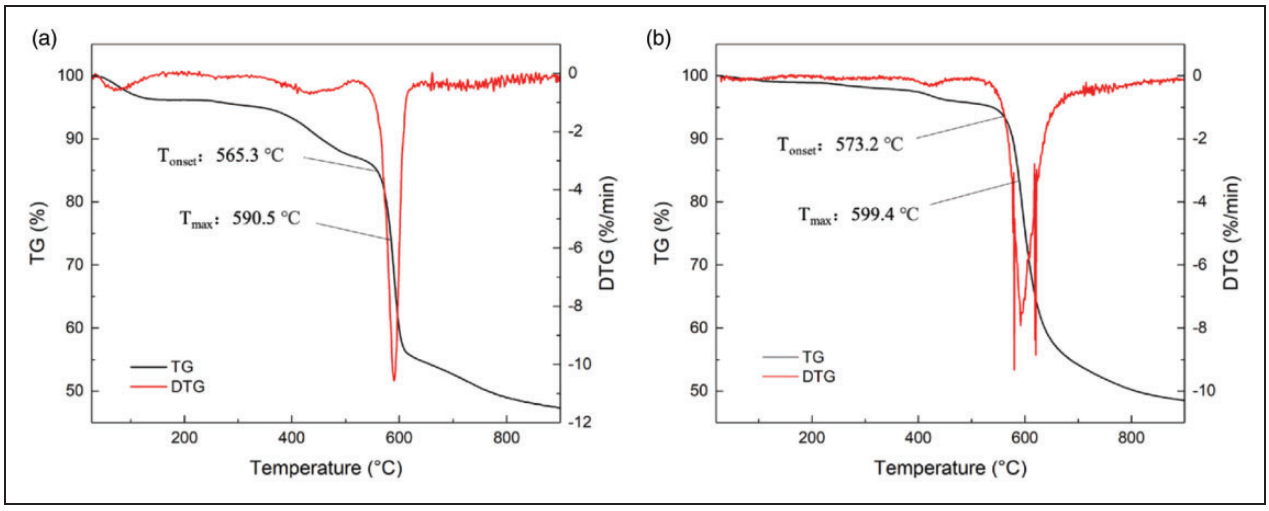

Figure 4. Thermogravimetry (TG) and differential thermal gravimetry (DTG) curves of fabrics in N_2 atmosphere: (a) Kevlar/polybenzimidazole fabric (a); (b) polyimide/Kevlar fabric (b). T_{onset} (°C): the onset degradation temperature; T_{max} (°C): the temperature at which thermal degradation rate was maximum.

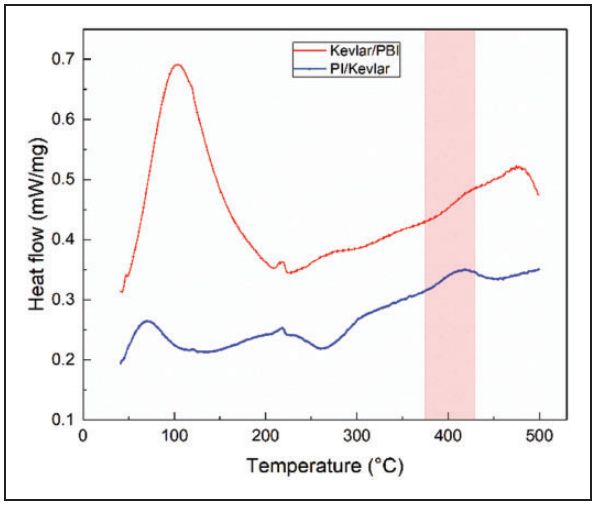

Figure 5. Differential scanning calorimetry curves for the Kevlar/polybenzimidazole (PBI) and polyimide (PI)/Kevlar.

outstanding thermal stability. According to the results of the TGA, it was expected that after the temperature reaches 500°C, the fabric would begin to pyrolyze rapidly, and the performance would begin to change significantly. For fabric A, the fabric was only slightly degraded (4–5%) when the temperature was lower than 400°C.

Microstructure changes after thermal aging

The aging specimens under the conditions of 30 and 60 kW/m^2 were selected, and a SEM study was carried out to observe the changes of the fabric during the thermal aging process from the microscopic level, as shown in Figure 6, where the images were focused at a magnification level of 1000× magnification (left) and 3000× high magnification (right) to observe the aging history of the fabric and compare it with the unaged ones. The degradation and microstructure change between Kevlar/PBI and PI/Kevlar fabrics were similar.

When fabric A was exposed to the heat flux level of 30 kW/m^2, charring appeared on the fiber surface. Although Figure 7 showed that the backside temperature of the fabrics did not exceed 300°C, several fiber surfaces showed greater damage in Figure 6. The microstructure began to show branching, accompanied by certain cracks after 27 s. Under 60 kW/m^2 heat flux, the fabric showed evidence of cracking after 2 s. The fiber began to be carbonized in a large area and broke directly after 15 s, which would lead to the significant decline of the mechanical properties.

The microstructure of fabric B begins to show branching under 30 kW/m^2 after 13 s. However, tensile strength results do not indicate significant damage. This may indicate that initial low-level heat flux exposures only cause surface microstructure damage and leave the body of the fiber relatively intact.[24] The brittleness of the microstructure appears to increase with increased duration time. Cracking continues to increase after 25 s at the 30 kW/m^2 (Figure 6, fabric B, 30 kW/m^2, 25 s), and some of them were also brittle. When fabric B was exposed to 60 kW/m^2, most of the structure has been reduced to ash after 12 s. These fibers also appear very brittle and have a jagged, broken appearance. These micro-level fiber damages could compare well to the result of fabric tensile strength after thermal aging.

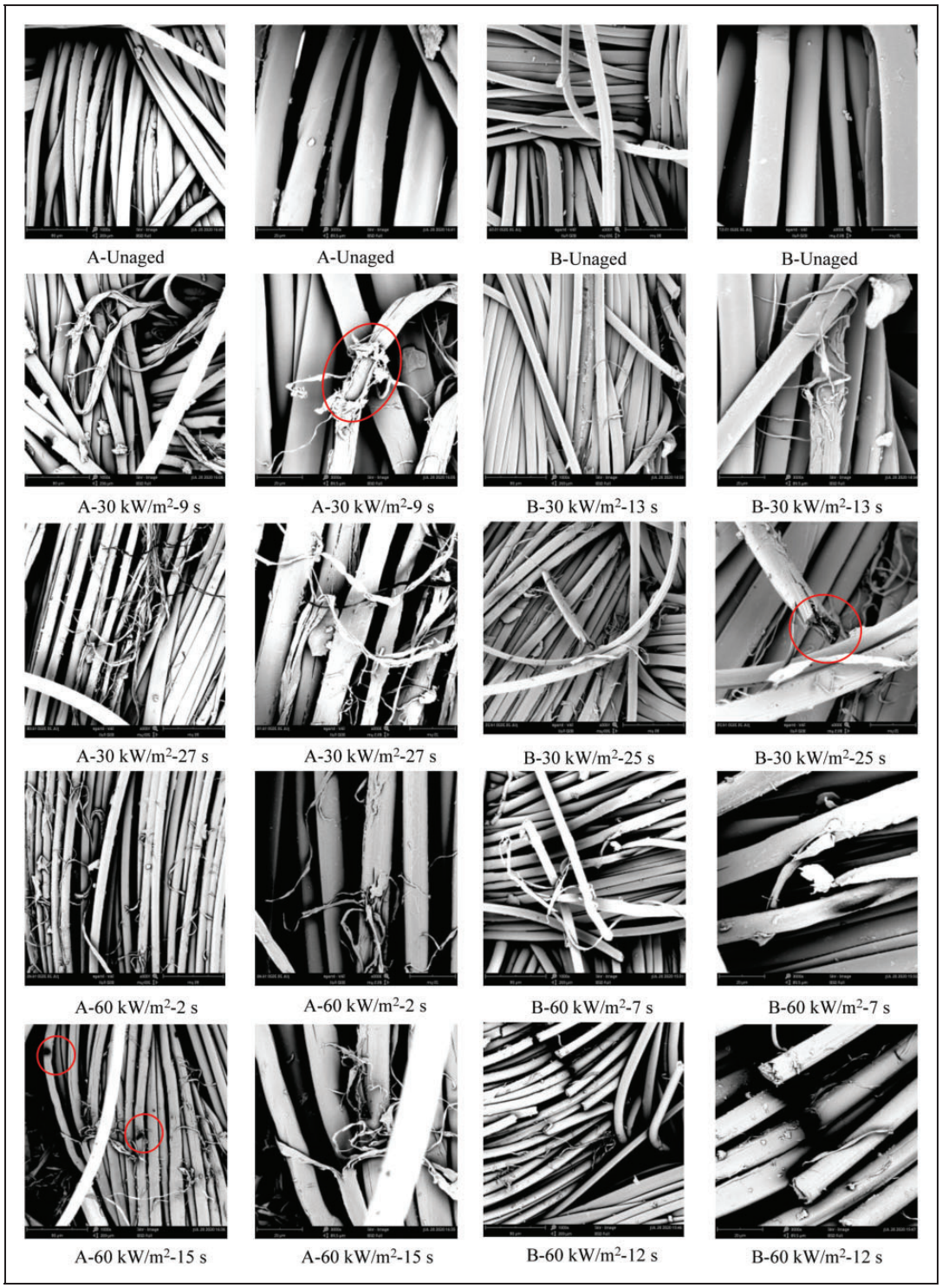

Figure 6. Images of the fabrics under the 1000× (left) and 3000× (right) scanning electron microscopy. A: Kevlar/polybenzimidazole fabric; B: polyimide/Kevlar fabric.

The result of the SEM analysis demonstrated that fiber damage at the microscopic level of the fabric could explain the decrease of the mechanical properties of the fabrics after thermal aging, which was mainly attributed to the carbonization and the development of cracks in the fiber structure. Studies have shown that the degradation of the fabric was consistent with the changes in the microstructure. The thermal aging

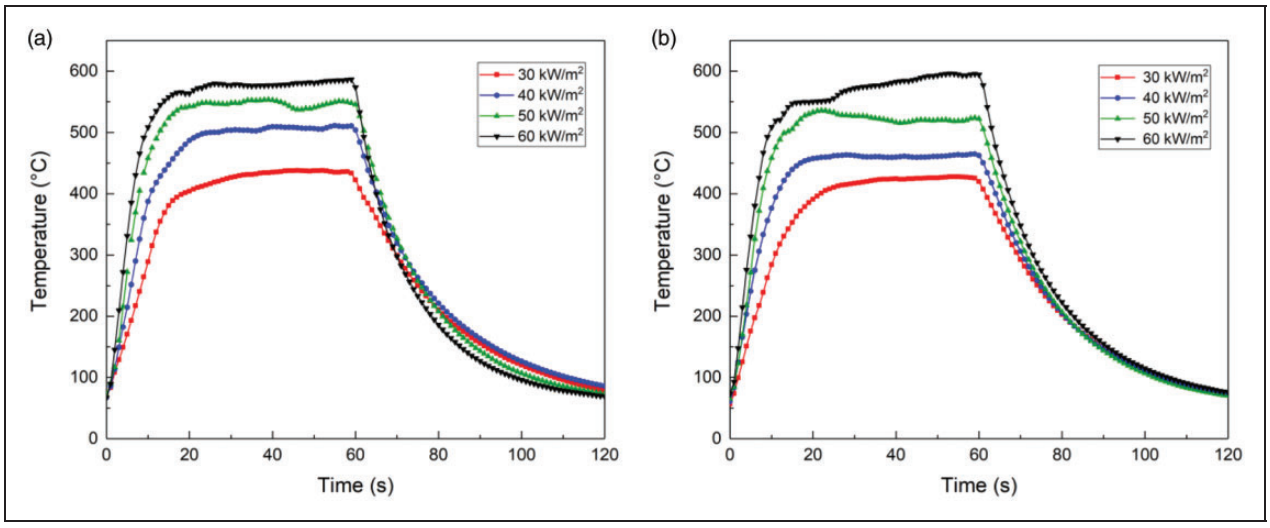

Figure 7. The 120 s temperature history of the backside of the outer shell during flame exposure (a) Kevlar/PBI fabric (A); (b) PI/Kevlar fabric (B).

process leads to dramatic changes in the fiber, and the main reason for the decrease in mechanical properties was the development of cracks in the fiber structure. The process started with the initiation of surface cracks and was subject to higher heat flux or longer heat exposure time. The cracks began to grow larger, which might cause the fiber bundles to separate. The development of fiber cracks on the microstructure and the carbonization process could explain why the performance of the fabric decreases after thermal aging. Figure 8 reveals the propagation stage of cracks in the fiber and the fiber tearing caused by carbonization of the surface.

According to the temperature profile on the backside of the fabrics, the degradation temperature was reached after about 14 s under the heat flux of 30 kW/m^2, and the time was 6 s under the heat flux of 60 kW/m^2. The degradation phenomenon of fabric B was not very obvious before 400°C (4–5%). When it was exposed to 30 kW/m^2, the temperature of the backside reached a stable state before serious degradation. The temperature of fabric B exposure to 60 kW/m^2 slightly increased after being heated for 20 s, which might be due to the charring of the fabric during heat exposure, and the fabric began to become brittle. Heat enters the interior of the fabric system through cracks formed on the surface of the fabric. Since the degradation of the fabric would affect its performance, understanding the temperature profile of the fabric under a heat flux could help explain the change in the mechanical strength after a specific heat exposure time.

Temperature profiles during flame exposure

Figure 7 shows the temperature history during flame exposure (60 s) at a specific heat flux and 60 s of temperature drop after leaving the fire source. The shutter was closed during the test, but the flame would also conduct a certain amount of heat transfer to the specimen through the shutter, which was why the temperature of the specimen was higher than room temperature at the beginning of the experiment.[24] For the temperature on the inner surface of the outer shell, all the curves exhibited similar change trends. The temperature increased rapidly during the first 20 s of exposure, and then gradually increased as the exposure continued. Figure 7 indicates that the time required for the specimens to reach the steady-state temperature is 20 s for both fabrics A and B. For any heat exposure exceeding 20 s, the temperature of the specimens remains basically constant.

Mechanical properties after flame exposure

Figure 9 illustrates the tensile strength of the samples after exposure to different levels of heat fluxes. The dotted line represents the minimum tensile strength requirement (623 N) of the outer shell fabric of the firefighters' protective clothing specified in NFPA 1971. Generally, as the exposure time increased, the tensile strength showed a downward trend. The fitting equation of the heat exposure time and the tensile strength of the fabric after thermal aging is shown in Table 3. If the heat exposure time under different heat flux densities is known, the tensile strength of the fabric at this time can be obtained according to the equations.

The flame exposure decreased the tensile strength of the specimens. Figure 9 illustrates that although the overall tensile strength shows a downward trend, in some cases, the tensile strength temporarily increases

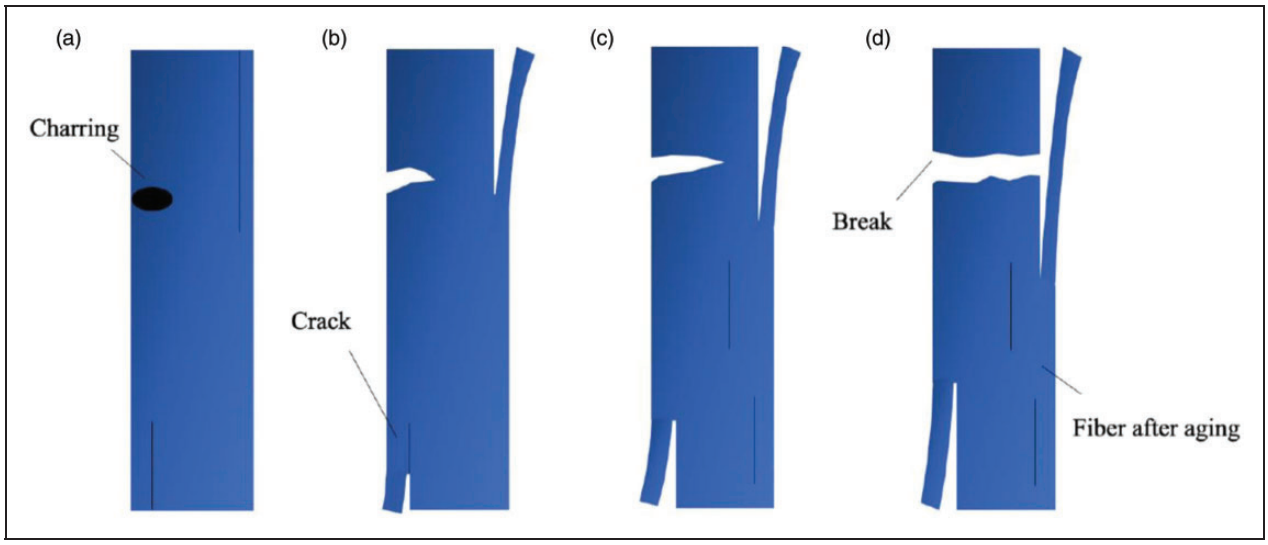

Figure 8. Crack propagation stage of fiber after aging (a) charring, crack initiation (b) and (c) partial thickness crack propagation and (d) fiber break resultant from increasing thermal aging exposure. conditions.

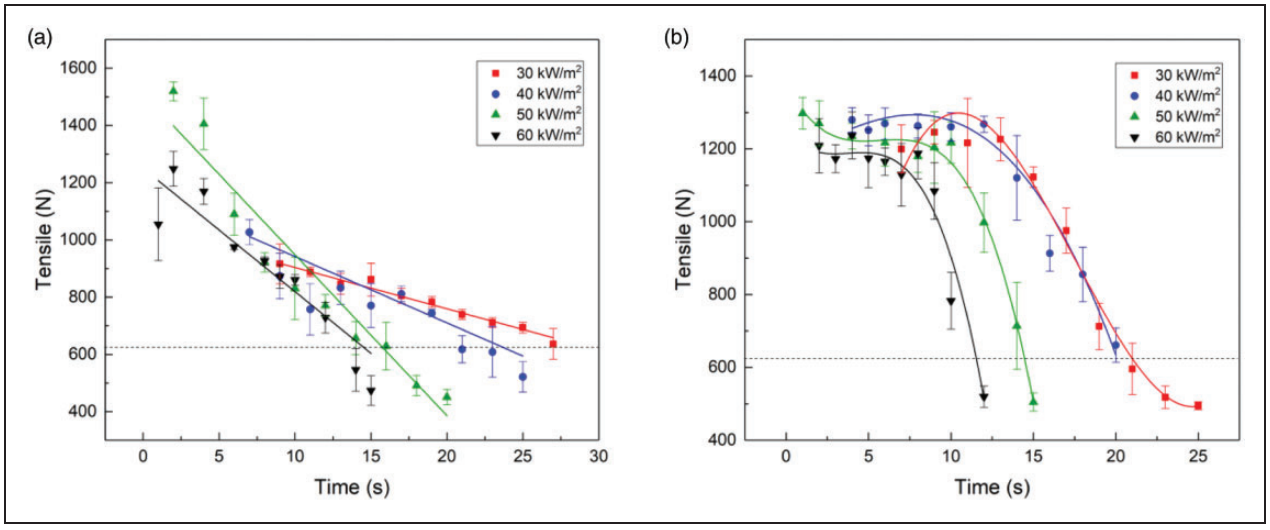

Figure 9. Tensile strength of fabrics after flame exposure: (a) Kevlar/polybenzimidazole fabric (A); (b) polyimide/Kevlar fabric (B).

after exposure. This increase was probably due to the uncertainty of the results, or complex cross-linking reactions between molecules, which increased the tensile strength of the fabric.[32] The tensile strength of the Kevlar/PBI fabric gradually decreased with the increase of heat exposure time, while the tensile strength of the latter would not change remarkably at the initial heat exposure, but dropped suddenly after a period of time. The higher tensile strength and stability for fabric B was attributed to the higher proportion of PI. The decrease of the tensile strength due to thermal aging was in good agreement with previous studies.[6,33] Furthermore, the tensile strength of fabric A shows a gradual decrease with the increase of heat exposure time, and in this case, even after 27 s of exposure from 30 kW/m^2, the tensile strength of the fabric still meets the requirements of NFPA 1971 for the outer shell. This was not difficult to explain, as the temperature of fabric A reaches about 400°C, at which temperature the degradation of the fabric was not obvious. In conjunction with Figure 7, when exposed to 30 kW/m^2, the temperature of the backside of the fabric reaches about 400°C. At this temperature, the fabric had not undergone serious degradation, resulting in its tensile strength still meeting the requirements. Therefore, if the fabric was damaged more severely, more exposure time or increased heat flux density was required. For fabrics exposed to lower heat flux, the decrease in

Table 3. Empirical equations for tensile strength of the fabric after flame exposure

Heat flux (kW/m^2)	Kevlar/PBI	R^2	PI/Kevlar	R^2
30	$Y=-14.44x+1048.2$	0.99	$Y=435.84x-29.7x^2+0.56x^3-656.5$	0.99
40	$Y=-23.18x+1173.69$	0.85	$Y=28.07x-0.53x^2-0.11x^3+1158.94$	0.93
50	$Y=-56.23x+1510.61$	0.94	$Y=-87.65x+15.86x^2-0.93x^3+1379.18$	0.99
60	$Y=-43.1x+1250.31$	0.88	$Y=-51.09x+14.2x^2-1.25x^3+1245.84$	0.98

PBI: polybenzimidazole; PI: polyimide.

Table 4. Correlation between tensile strength and different fabric parameters

Parameter	Correlation coefficient (r)	P-value
T_k	0.438	0.000*
Hf	0.205	0.000*
Ws	0.438	0.000*
t	–0.784	0.000*
T	–0.778	0.000*
T_g	–0.438	0.000*
T_d	0.438	0.000*

T_k: thickness, mm; Hf: heat flux, kW/m^2; Ws: weave structure; t: exposure time, s; T: the temperature on the backside of fabric, °C; T_g: glass transition temperature, °C; T_d: the degradation temperature, °C.
*: the correlation is significant at 0.01 level.

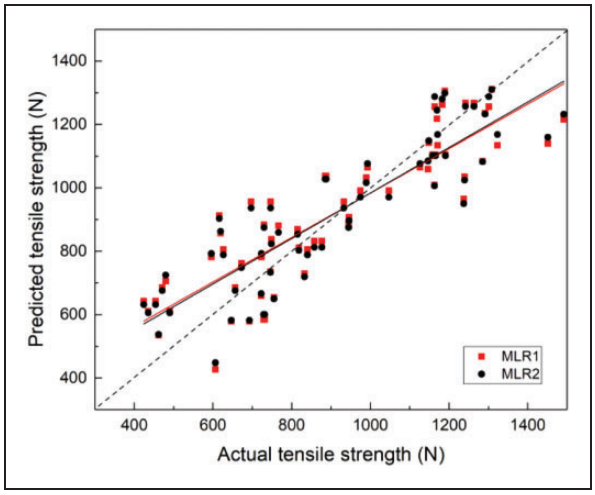

Figure 10. Comparison of predicted data with experimental data for tensile strength. MLR1: T, T_g, T_d are not included in the input parameters; MLR2: input parameters include T, T_g, T_d.

tensile strength was mainly due to the increase in exposure time.

Models for predicting the tensile strength of the fabrics after flame exposure

MLR model. In order to develop a model with better predictive performance, the key properties that affect the tensile strength of flame-retardant fabrics after thermal aging were determined. In the correlation analysis, the weight was considered as a constant (200 g/m^2) and was excluded. The P-value shown in Table 4 indicates that all the selected indicators are significantly related to the tensile strength of the fabric after thermal aging. The most important factor affecting thermal aging of the fabrics is the heat exposure time, followed by the surface temperature during thermal aging. It is known that long-term heat exposure and temperature rise increase the thermal aging of the fabrics, so the tensile strength would be significate changed. Heat flux is an important factor affecting thermal aging of the fabrics; however, its r-value is only 0.205. This may be due to the narrow range of heat flux selected in this study. On the other hand, it also reflects the limitations of the MLR model such that it depends on the relationship between the data, and remodeling is needed for newly added variables to perform predictions.[31]

According to the r-value, the macro index of the fabric was used as the input parameter (t, Hf, T_k, Ws), and the output model is shown in Equation (6). Here, T_k was excluded because it was co-linear with Ws. The model's R^2 is 0.76 and RMSE is 138.61. In order to explore whether the addition of T, T_g and T_d would affect the performance of the model, these indicators were added as the input parameters of the model. The prediction model is shown in Equation (7) with R^2 of 0.77 and RMSE of 134.89. Here, T_g was excluded since it was co-linear with T_d; Ws and T_k were excluded, which may be because these fabric parameters become less important after the temperature parameter was added

$$S=-37.82t-8.138Hf+121.73Ws+1576.48 \quad (6)$$

$$S=-32.31t-6.42Hf+15.3T_d-0.245T-7015.03 \quad (7)$$

where S is the tensile strength, N; t is the exposure time, s; Hf is the heat flux, kW/m^2; Ws is the weave structure of the fabric; T_d is the degradation temperature, °C; T is the temperature on the backside of fabric, °C.

Figure 10 illustrates the comparison between the predicted value of the model and the actual value of the experiment. If the predicted value of the model is exactly the same as the actual value, the predicted and actual value of the tensile strength will lie on the diagonal, which is represented by a dotted line in Figure 10. The closer the slope of the fitted curve is to the dotted line, the better the prediction accuracy will be. Figure 10 shows the influence of the addition of fabric characteristic index (T, T_g, T_d) on the MLR model performance. When statistical modeling methods were used, the addition of these indexes has no remarkable influence on the predictive ability of the model. The reason was that simple linear regression cannot detect the complicated mathematical relationship between various parameters. Therefore, a more powerful model was needed to analyze such problems.

ANN model. The ANN model reaches a higher coefficient of determination (R^2) value and lower prediction error (RMSE) than that of the MLR model. In terms of accuracy, the ANN model was better than the MLR model in predicting the tensile strength of the fabric after flame exposure. The prediction performance of the ANN model developed is presented in Table 5.

Table 5. The R^2 and root mean square error (RMSE) of the artificial neural network (ANN) model

Models	R^2	RMSE
ANN1	0.88	96.91
ANN2	0.92	81.92

Note: ANN1: the model does not contain T, T_g, T_d parameters; ANN2: the model contains T, T_g, T_d parameters.

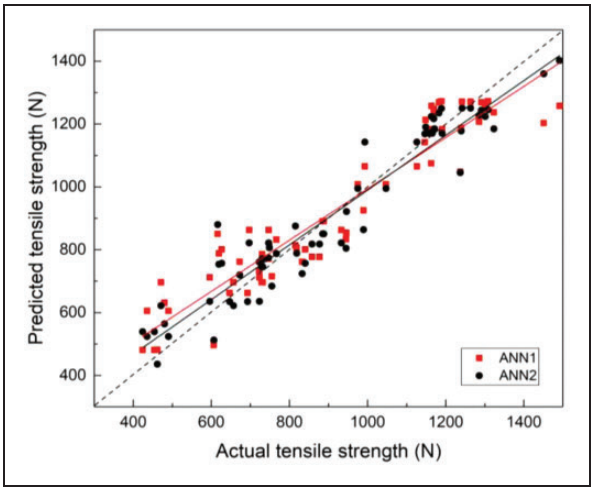

Figure 11. Comparison of predicted data with experimental data for tensile strength. ANN1: T, T_g, T_d are not included in the input parameters; ANN2: input parameters include T, T_g, T_d.

Figure 11 shows the influence of the addition of the fabric characteristic index (T, T_g, T_d) on the ANN model performance. For the ANN model (ANN1) without the temperature rise feature index (T, T_g, T_d) in the input parameters, the R^2 is 0.88 and RMSE is 96.91. These two indexes of ANN2 with the addition of the above three indicators (T, T_g, T_d) is 0.92 and 81.92, respectively. This demonstrated that the addition of the fabric temperature rise characteristic index could improve the prediction accuracy of the ANN model. The slope of the data fitting curve predicted by the ANN2 model is closer to the diagonal line.

Comparison of MLR and ANN models. An important role in this study is the possibility to predict the lifetime of firefighters' protective clothing after flame exposure, which is associated with a safety limit for the user.[7] Regardless of whether the characteristic index (T, T_g, T_d) of fabric temperature rise was added to the input parameters, the predictive performance of the ANN model was higher than that of the MLR. The possible reason for the difference in accuracy might be that the temperature change of the fabric during the flame exposure process leads to the deterioration of the fabric micro-level. Therefore, the temperature rise index is an important factor that cannot be neglected to improve the predictive accuracy of thermal aging for flame-retardant fabrics.

Previous studies reported that the high-performance materials used to manufacture fire protective clothing were sensitive to the environmental agents to which the clothing was exposed in service.[34] Results demonstrated that flame exposure decreased the tensile strength. The decrease in performance was attributed to the fact that thermal aging promotes carbonization, cracks, and breaks on the fiber surface, resulting in a decrease of tensile strength. A prediction model study revealed that the addition of the fabric temperature rise characteristic index (T, T_g, T_d) could improve the prediction accuracy of the model. When establishing a predictive model, the temperature rise characteristic indexes of the fabric were also important factors that should be considered in addition to the macro-indices of the fabric.

Conclusion

The mechanical properties of the flame-retardant fabrics of common firefighting clothing after flame exposure were studied, and their thermal degradation phenomenon was explained in the current study. Progressive development of microstructure cracks and holes could be the cause of decreased tensile strength after thermal aging. Increased thermal aging caused the increasing brittle nature of individual textile fibers. In

the research of using MLR and ANN models to predict the tensile strength of fabrics after flame exposure, the MLR model presented worse performance ($R^2 = 0.76$, RMSE = 138.61) than the ANN model ($R^2 = 0.88$, RMSE = 96.91) when using thickness, heat flux, weave structure, and exposure time as the input parameters. The addition of T, T_g and T_d in the model could improve the prediction accuracy. For the MLR model, the addition of T, T_g, and T_d has no significant impacts on the prediction accuracy of the model. The R^2 of the model was only increased by 1%, and the RMSE was reduced by 3.72. As regarding the ANN model, the addition of temperature indicators increased R^2 by 4% and reduced RMSE by 14.99, which was recommended to predict the tensile strength of the fabric after thermal aging. The study provides theoretical support for the thermal aging and degradation of flame-retardant fabrics and will help to evaluate the service life of the thermal protective clothing.

Declaration of conflicting interests

The author(s) have no conflicts of interest to declare.

Funding

The author(s) disclosed receipt of the following financial support for the research, authorship, and/or publication of this article: This work was supported by the Chenguang Program supported by, the Fundamental Research Funds for the Central Universities (Grant No. 2232021G-08), Shanghai Education Development Foundation and Shanghai Municipal Education Commission (Grant No. 18CG76). and Shanghai Summit Discipline in Design (Grant No. DA19202).

ORCID iDs

Xiaohan Liu https://orcid.org/0000-0001-8811-7884
Miao Tian https://orcid.org/0000-0001-8726-5156
Jun Li https://orcid.org/0000-0001-6805-4521

References

1. Nayak R, Houshyar S and Padhye R. Recent trends and future scope in the protection and comfort of fire-fighters' personal protective clothing. *Fire Sci Rev* 2014; 3: 4.
2. Raimundo M and Figueiredo AR. Personal protective clothing and safety of firefighters near a high intensity fire front. *Fire Safe J* 2009; 44: 514–521.
3. Tian M, Wang Q, Xiao YT, et al. Investigating the thermal-protective performance of fire-retardant fabrics considering garment aperture structures exposed to flames. *Material* 2020; 13: 3579.
4. Rezazadeh M. *Evaluation of performance of in-use firefighters' protective clothing using non-destructive tests*. Saskatchewan: University of Saskatchewan Saskatoon, 2013.
5. Song G, Barker RL, Hamouda H, et al. Modeling the thermal protective performance of heat resistant garments in flash fire exposures. *Text Res J* 2014; 74: 1033–1040.
6. Rezazadeh M and Torvi DA. Assessment of factors affecting the continuing performance of firefighters' protective clothing: a literature review. *Fire Technol* 2011; 47: 565–599.
7. Lu Y, Wang L and Gao Q. Predicting tensile strength of fabrics used in firefighters' protective clothing after multiple radiation exposures. *J Text I* 2018; 109: 338–344.
8. Mandal S and Song G. An empirical analysis of thermal protective performance of fabrics used in protective clothing. *Ann Occup Hyg* 2014; 58: 1065–1077.
9. Nazare S, Davis RD, Peng JS, et al. Accelerated weathering of firefighter protective clothing: delineating the impact of thermal, moisture, and ultraviolet light exposures, *National Inst Stand Technol* 2012; 6: 113–129.
10. Moezzi M and Ghane M. The effect of UV degradation on toughness of nylon 66/polyester woven fabrics. *J Text I* 2013; 104: 1277–1283.
11. Feng QQ, Zhu FL and Hu JF. Estimation of the radiant performance of flame-retardant fabrics considering thermal degradation effect. *J Eng Fibers Fabrics* 2019; 14: 1–10.
12. Xing ZX and Jiang JC. The model of radiated heat flux from pool fire to the surface of tanks. *Petrochem Equip* 2004; 33: 18–20.
13. Rossi RM, Bolli W and Stampfli R. Performance of firefighter's protective clothing after heat exposure. *Int J Occup Safe Ergon* 2008; 14: 55–60.
14. Vogelpohl TL. *Post-use evaluation of firefighter's turnout coats*. Lexington, KY: University of Kentucky, 1996.
15. Cui ZY, Ma CJ and Lv N. Effects of heat treatment on the mechanical and thermal performance of fabric used in firefighter protective clothing. *Fiber Text Eastern Eur* 2015; 23: 74–78.
16. Lu Y, Li J, Li X, et al. The effect of air gaps in moist protective clothing on protection from heat and flame. *J Fire Sci* 2013; 31: 99–111.
17. Iyer RV, Sudhakar A and Vijayan K. Decomposition behavior of Kevlar 49 fibres: Part II. At T values < Td. *High Perform Polym* 2006; 18: 495–517.
18. An SK, Barker RL and Stull JO. Flammability measurement and thermal aging of chemical protective suit materials. *Soc Fiber Sci Technol Jpn* 1999; 55: 10.
19. Udayraj P, Talukdar A, Das R, et al. Estimation of radiative properties of thermal protective clothing. *Appl Ther Eng* 2016; 100: 788–797.
20. Camenzind MA, Dale DJ and Rossi RM. Manikin test for flame engulfment evaluation of protective clothing: historical review and development of a new ISO standard. *Fire Mater* 2007; 31: 285–295.
21. Pal SK, Thakare VB, Singh, G, et al. Effect of outdoor exposure and accelerated ageing on textile materials used in aerostat and aircraft arrester barrier nets. *Ind J Fibre Text Res* 2011; 36: 145–151.
22. Robinson JW, Frame EMS and Frame GM. *Undergraduate instrumental analysis*. New York: Marcel Dekker Incorporated, 2005.

23. Zhang XS, Tang XN, Wang R, et al. The fire-retardant properties and pyrolysis mechanism of polysulfonamide (PSA) fibers. *Text Res* J 2017: 88: 1299–1307.
24. Fulton M. *Evaluating the performance of thermally and UV aged firefighters' protective clothing using both destructive and non-destructive method*. Saskatchewan: University of Saskatchewan Saskatoon, 2017.
25. Mandal S, Annaheim S, Greve J, et al. Modeling for predicting the thermal protective and thermo-physiological comfort performance of fabrics used in firefighters' clothing. *Text Res J* 2018; 89: 2836–2849.
26. Zaefizadeh M, Khayatnezhad M and Gholamin R. Comparison of multiple linear regression (MLR) and artificial neural networks (ANN) in predicting the yield using its components in hulless barley. *Am Eur J Agric Environ Sci* 2011; 10: 60–64.
27. Hui CL and Ng SF. Predicting seam performance of commercial woven fabrics using multiple logarithm regression and artificial neural networks. *Text Res J* 2009; 79: 1649–1657.
28. Dursun M and Senol Y. Neural network based thermal protective performance prediction of three-layered fabrics for firefighter clothing. *Ind Text* 2019; 70: 57–64.
29. Ahmad MW, Mourshed M and Rezgui Y. Trees vs neurons: comparison between random forest and ANN for high-resolution prediction of building energy consumption, *Energy Build* 2017; 147: 77–89.
30. Lacuna Y, Bengio Y and Hinton G. Deep learning. *Nature* 2015; 521: 7553.
31. Mandal S. *Studies of the thermal protective performance of textile fabrics used in firefighters' clothing under various thermal exposures*. Edmonton: University of Alberta, 2016.
32. Jane MFP, Michelle L and Costa MCR. Evaluation of thermal stability and glass transition temperature of different aeronautical polymeric composites. *Polym Plastics Technol Eng* 2006; 45: 157–164.
33. Aidani RE, Dolez PI and Vukhanh T. Effect of thermal aging on the mechanical and barrier properties of an e-PTFE/Nomex® moisture membrane used in firefighters' protective suits. *J Appl Polym Sci* 2011; 121: 3101–3110.
34. Dolez PI, Tomer NS and Yassine MA. Quantitative method to compare the effect of thermal aging on the mechanical performance of fire protective fabrics. *J Appl Polym Sci* 2018; 136: 47045.